Taylor & Francis
Taylor & Francis Group

Numerical Heat Transfer, Part A: Applications
An International Journal of Computation and Methodology

ISSN: 1040-7782 (Print) 1521-0634 (Online) Journal homepage: http://www.tandfonline.com/loi/unht20

Heat transfer and thermodynamic processes in coal-bearing strata under the spontaneous combustion condition

Yanming Wang, Guoqing Shi & Zhixiong Guo

To cite this article: Yanming Wang, Guoqing Shi & Zhixiong Guo (2017) Heat transfer and thermodynamic processes in coal-bearing strata under the spontaneous combustion condition, Numerical Heat Transfer, Part A: Applications, 71:1, 1-16, DOI: 10.1080/10407782.2016.1243978

To link to this article: http://dx.doi.org/10.1080/10407782.2016.1243978

NUMERICAL HEAT TRANSFER, PART A
2017, VOL. 71, NO. 1, 1–16
http://dx.doi.org/10.1080/10407782.2016.1243978

Taylor & Francis
Taylor & Francis Group

Heat transfer and thermodynamic processes in coal-bearing strata under the spontaneous combustion condition

Yanming Wang[a,b], Guoqing Shi[a,b], and Zhixiong Guo[b]

[a]School of Safety Engineering, China University of Mining and Technology, Xuzhou, Jiangsu, P. R. China; [b]Department of Mechanical and Aerospace Engineering, Rutgers, The State University of New Jersey, Piscataway, New Jersey, USA

ABSTRACT

Simulations and experiments have been carried out to investigate heat transfer and thermodynamic processes in coal-bearing strata in order to quantitatively understand the development of underground coal fires under the spontaneous combustion condition. With the controlled temperature and under lean oxygen conditions, the thermodynamic parameters for coal oxidation at different stages are experimentally determined in combination with the simultaneous thermal analysis. A combined heat transfer model of conduction, convection, and radiation with finite reactions is developed for the porous coal and rocks. The temperature distributions in the coal and roof strata at different times are simulated based on the single- and two-stage kinetic models, respectively, and compared with field geophysical prospecting. Effects of oxidation kinetic properties due to coal metamorphism on propagation of coal fires are examined. It reveals that a significant step change exists during the thermal process of coal fire caused by two-stage oxidation, and the coal rank of occurrence directly determines the spontaneous combustion period of underground coal fire.

ARTICLE HISTORY
Received 7 June 2016
Accepted 16 September 2016

1. Introduction

Underground coal fires caused mainly by spontaneous combustion are a global problem threatening the environment and occupational health [1]. As a severe disaster, its prime impacts include toxic and greenhouse gas emission, ecological destruction by high temperature, resources waste, and geomorphic effects with land subsidence and cracks [2], to name a few. In the past decade, the phenomena of coal fires and spontaneous combustion have been widely investigated and comprehensively understood from both the microscale and large-scale aspects.

Previous researches on the initiation of self-heating [3] recognized the mechanism of coal spontaneous combustion as the oxygen experiencing four stages: physical adsorption of oxygen, chemical adsorption, decomposition of oxygenated hydrocarbons, and self-ignition during temperature increasing period [4]. After the coal and oxygen reaction process, gaseous products such as carbon monoxide, carbon dioxide, and water vapor are released. Thus, coal spontaneous combustion can be regarded as an exothermic reaction of coal and oxygen as follows:

$$\text{Coal} + \text{O2} \rightarrow \text{Solid Products} + \text{Exhausted Gases} + \text{Heat Release} \quad (1)$$

In recent years, studies in the field of coal spontaneous combustion mainly focused on heat release [5], gas products [6], functional groups, and free radicals changes at low-temperature oxidation state [7], etc. Meanwhile, combustion and pyrolysis characteristics at high temperature are of great interest

CONTACT Yanming Wang and Zhixiong Guo guo@jove.rutgers.edu; cumtwangym@163.com Department of Mechanical and Aerospace Engineering, Rutgers, The State University of New Jersey, Piscataway, NJ 08854, USA.
Color versions of one or more of the figures in the article can be found online at www.tandfonline.com/unht.

Nomenclature

A	frequency factor, Hz	t	time, s
C_o	local oxygen concentration, kg/m^3	T	absolute temperature, K
C_p	specific heat, kJ/(kg · K)	v	seepage velocity, m/s
D	diffusion coefficient of oxygen air, m^2/s	w	quantity of local oxygen consumption. Kg/(m^3 · s^1)
E_a	activation energy, kJ/mol		
$\bar{g}$	gravitational vector, m/s^2	β	attenuation coefficient, m^{-1}
k	permeability, m^2	σ	Stephan–Boltzmann constant
O_r	theoretical oxygen requirement for combustion, kg/kg coal	λ	thermal conductivity, W/(m · K)
		μ	air dynamic viscosity, Pa · s
p	hydrostatic pressure, Pa	ρ	density, kg/m^3
S	compressibility, 1/Pa	φ	porosity
q	heat release rate, W/g		
q_r	heat flux of radiation, W/m^2	***Subscripts***	
Q	reaction heat, J/g	c	remaining coal
Q_{net}	net calorific value of coal, MJ/kg	f	leakage air
R	gas constant	s	solid material

in energy chemical industry [8]; and kinetic properties such as initial reaction and ignition temperature [9], reaction rate [10], and their relationships have been studied intensively [11].

However, the occurrence of coal fires depends on not only the coal itself but also the physical state as well as geological structures and leakage airflow paths. Many theoretical and modeling investigations have been carried out to understand the physical and chemical processes of coal fires including the seepage in fractures [12], oxygen consumption [13], products diffusion [14], heat transfer [15], thermal anomaly, and fire front propagation [16]. These studies reported that the development of coal oxidation requires a large surface area of crushed material as well as a slow migration of air through which spontaneous combustion of underground coal usually takes place in the collapsed zones or pillar edges [17] and occurs through an extreme complex interactions among thermal, hydraulic, chemical, and mechanical processes [18].

Emphasis of existing numerical studies on coal fire development was primarily placed on understanding the relationship of seepage flow, diffusion, and heat transfer in macroscale. For heat release during coal oxidation, it was usually assumed as a one-step reaction or was reduced to a constant thermal source and set the point of initial ignition with high temperature artificially [19]. Unfortunately, such simplified assumptions may cause the ignition occurring prematurely and the thermodynamic development of coal fires are not accurately estimated in terms of temperature prediction. Geophysical field surveys have evidenced that mined coal seam starts to burn several decades after uncovering and the combustion activity slightly increases in a long-term period [20]. Modeling results could hardly be consistent with field observation without employing a real kinetic model for coal oxidation.

Hence, it is critical to develop a full-size simulation of thermodynamic process of coal spontaneous combustion in coupling with better kinetic model for coal oxidation. To this end, the mass variation and heat release during coal oxidation at different stages and temperatures will be first measured in this study using the combined thermogravimetric (TG) [21] and differential scanning calorimetry (DSC) apparatus [22] which enable real-time record of a series weight and heat changes caused by coal oxidation and pyrolysis reaction with elevated temperature. This will reveal the whole history of coal fire development from oxygen adsorption to fuel burnout and enhance understanding the correlations between microscale kinetic properties of coal oxidation and heat transfer in the large-scale medium. Based on the experimental results of synchronous thermal analysis for a typical coal sample, a two-stage oxidation model as well as the relevant kinetic parameters including the activation energy, reaction frequency and heat, and threshold temperatures are then obtained by the fitting method. After that, a two-dimensional combined conduction, convection, and radiation heat transfer model is established with finite reaction for heat and mass transfer simulation of coal

fires in a porous subsided medium and with appropriate initial and boundary conditions. The heat release rate for coal oxidation in each step of the two-stage kinetic model will be employed as a temperature-dependent thermal source to predict temperature distributions and to investigate thermodynamic process of coal spontaneous combustion in mined coal-bearing strata. Finally, the numerically predicted results will be validated with field geophysical surveys in an open pit coalfield, and compared with results obtained by using the classified kinetic model. Since coal self-ignition depends on coal types [23], we will analyze three coal samples with different ranks and metamorphic grades in this study.

2. Experiments and kinetics analysis

2.1. Synchronous thermal analysis

Synchronous thermal analysis enables evaluation of heat evolved during the oxygen chemisorption process by relating the heat to the mass increase in the same temperature interval [24]. It is commonly used to acquire oxidation kinetic properties in coal spontaneous combustion. In this study, the synchronous thermal analysis was carried out by an SDT-Q600 instrument of TG and DSC measurements. A brief experimental procedure is described as follows:

1. Calibrations of weight, temperature, and sensitivity of the instrument.
2. About 8 mg of a vacuum-dried coal sample in the size range of 180–380 μm was placed in the reference crucible made of α-Al_2O_3. A high rank anthracite consisted of 85.35% fixed carbon was chosen as the typical sample involved in the present measurement.
3. The sample was first heated to 483 K in pure N_2 with a flow rate of 70 mL/min, held for 330 minutes to further drive off the moisture and followed by cooling down to 303 K.
4. Hybrid gas of ultra-pure O_2 and N_2 with 20% of O_2 was mixed with air of a flow rate of 100 mL/min. Beginning at 303 K, the sample was heated to 873 K with a constant heating rate of 1 K per minute, and the weight variation and heat evolution were recorded by the instrument synchronously.

The exothermal capacity of coal related to the reaction rate at different temperatures can be expressed by the Arrhenius equation [25]:

$$q(T) = QAe^{-E_a/RT} \tag{2}$$

where $q(T)$ is the heat release rate per unit mass at absolute temperature T, E_a and A are the activation energy and the frequency factor, respectively, depending on the coal rank and measurement method, R is the universal gas constant, and Q is the reaction heat.

Three kinds of typical coal obtained from different coalmines are considered in this study, including a high volatile lignite (Coal A), a bituminous coal (Coal B), and a high-carbon content anthracite (Coal C). The profiles of weight (denoted as TG curve) and heat release rate (denoted as DSC curve) of coal sample C varying with temperature are illustrated in Figure 1 to show typical results from the TG–DSC test on nonisothermal oxidation of the coal sample.

According to the coal weight variation on the TG curve, the oxidation process of coal combustion could be divided into five stages, which are desorption weightlessness, chemisorption weightiness, thermal decomposition, combustion and burnout, by four critical temperatures including active temperature T_1, maximum weight temperature T_2, ignition temperature T_3, and burnout temperature T_5, and between, there exists a maximum weightless rate temperature T_4 as the key point for characterization of coal oxidation process.

There are two obvious peaks in the DSC curve as shown in Figure 1. The first one is the adsorption exothermic peak appearing in the process of oxygen adsorption and weight gain beginning from active temperature T_1. In fact, this peak temperature does not coincide with the maximum weight temperature T_2 on the TG curve. It proves that the first exothermic peak is not only due to oxygen adsorption heat release, but it also incorporates heat release from direct oxidation reactions at low

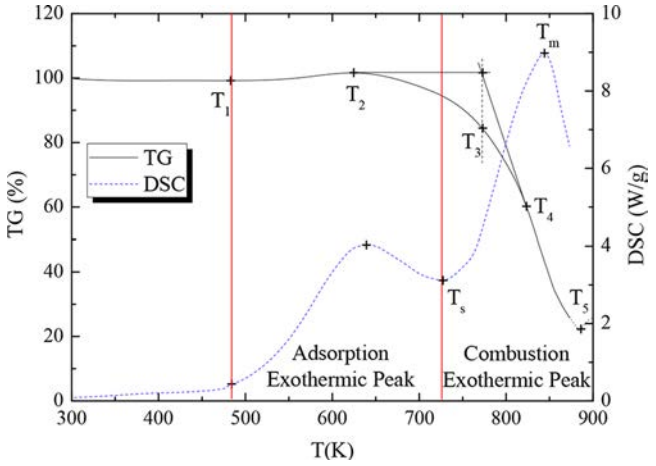

Figure 1. Profiles of TG–DSC measurement of sample Coal C.

rate. With increase of oxidation temperature, the chemical adsorption rate of the primary group decreases, while the endothermic decomposition rate increases rapidly, resulting in the overall performance of heat release decreases gradually until it reaches a local minimum at temperature T_s. The second peak in the DSC curve is named combustion exothermic peak, which is mainly derived from the chemical reactions of primary and secondary active groups in coal and combustion of fixed carbon in depolymerization products of gas volatile, liquid tar, and solid semicoke. At the end of the exothermic chemisorption process, the increasing secondary groups produced by decompositing intermediates from native groups adsorption coherently react. At the same time, when the temperature rises to exceed the ignition point, fixed carbon in glial coal particles formed by thermal decomposition begins to combust and releases great heat. Although endothermic pyrolysis occurs synchronously, the overall performance of heat release increases constantly until the heat release rate achieves maximum at temperature T_m, which is lower than the maximum weightless rate temperature T_4 but higher than burnout temperature T_5. The fixed carbon gradually reduces and the heat release rate decreases until the fuel burnout.

2.2. Two-stage kinetic model

Based on the exothermic process on the DSC curve from low temperature to burnout as shown in Figure 1, a two-stage kinetic model is established to directly relate the two main peaks which could represent the whole thermodynamic process for coal oxidation. One can reorganize Eq. (2) by natural logarithm processing as follows:

$$\ln\ q = -\frac{E_a}{R}\cdot\frac{1}{T} + \ln\ QA \tag{3}$$

Via plotting ln q against the reciprocal of temperature T obtained directly from a single heating rate test in the nonisothermal analysis (see the black curve in Figure 2), the values of kinetic parameters QA and E_a in the two-stage model could be directly obtained by the intercepts and slopes of the linearly fitting curves, respectively. For coal sample C measured from Figure 2, the activation energy E_a below and above the minimum temperature T_s (725 K) between two exothermic peaks are 61.2 and 92.9 kJ/mol, respectively; while the relevant values of QA are 3.8×10^5 and 1.0×10^7 W/g, respectively. It should be pointed out that when the heating temperature is beyond the threshold T_m that reads 844 K in the present single measurement, the reaction rate turns to decrease until fuel burnout. So the quantity of heat release rate was assumed constant after the combustion temperature rises to this critical value.

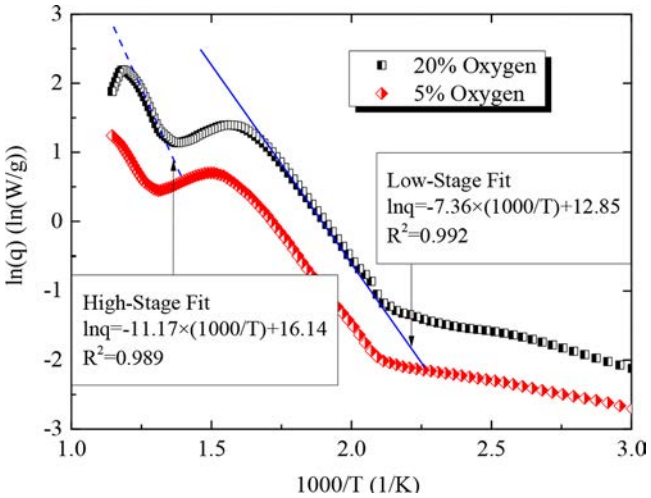

Figure 2. Determination of coal oxidation of Coal C for the two-stage kinetics under two different oxygen concentrations.

Furthermore, the reaction rate is predominated by the concentration of oxygen in the fire front area, which is mainly supplied by air convective transport through the fractures of overlying rocks. Considering the effects of supplemental oxygen on the thermodynamic development of coal spontaneous combustion, another single heating rate experiment with 5% of oxygen supply was carried out and the kinetic process is denoted by the red curve in Figure 2. Comparing the two results, it is clear that the heat release rate under rich oxygen condition (20%) is greater than that with lower oxygen supplement (5%) at any temperature. However, nearly same slopes of the fitted curves are yielded, and this demonstrates that the active energy does not change under different oxygen concentrations. Only the reaction rate decreases as the concentration of supplemental oxygen reduces. In this study, the monotonic decreasing rule is employed to describe the variation of kinetic parameter QA against the oxygen concentration. However, the critical temperatures T_{m} and T_{s} vary slightly under lean oxygen conditions. For the sake of simplicity, they are assumed constant in the present model. For context, the coal oxidation could not occur under lean oxygen condition when the concentration is lower than 5% in the simulation.

3. Numerical models

3.1. Mathematical formulation

The coupled diffusion-reaction-heat transfer phenomenon in porous medium [26] is used to develop the energy transport equation for temperature distribution in the coal and rock strata, along with specific boundary conditions and an initial condition. It assumes thermal equilibrium between the solid matrix and gas; and thus, the temperatures of gas and solid materials are regarded as the same. Thermal energy released in coal spontaneous combustion is transported through three mechanisms: heat conduction through surrounding rocks, convection through gas transport in the rocks, and thermal radiation due to high combustion temperature. Because coal oxidation is an exothermic process as mentioned in Section 2.1, a link between heat production and oxygen consumption must be taken into account. The density and thermal conductivity of coal or rock are much higher than those of gas. Considering all the factors aforementioned, a mathematical model combining the two-phase energy conservation equations is formulated as follows:

$$(1-\varphi)\rho_s C_{Ps}\frac{\partial T}{\partial t}+\rho_f C_{Pf}\vec{v}\cdot\nabla T=\nabla\cdot\left((1-\varphi)\lambda_s\nabla T-\vec{q_r}\right)+(1-\varphi)\rho_c q(T) \tag{4}$$

where t is the time, C_p is the specific heat, φ is the porosity in strata, ρ is the density, λ is the thermal conductivity, $\vec{v}$ is the velocity of seepage flow, $\vec{q_r}$ is the heat flux of radiation, and subscripts s, f, and c stand for the solid material (coal or rocks), leakage air, and the remaining coal, respectively.

Thermal radiation plays an important role in the heat transfer process under high temperature condition and the radiation heat flux should be solved by radiative transfer equation (RTE) [27]. In the present study, however, the radiative energies transferring in coal/rocks of high density extinct drastically and the strata can be regarded as an optically very thick medium [28]. This is different from the scattering behavior in a sparse particle system. Therefore, the diffusion approximation method is applied and the heat flux $\vec{q_r} = -(16\sigma T^3/3\beta)\nabla T$, in which σ ($= 5.67 \times 10^{-8}$ W/(m^2 K^4)) is the Stephan–Boltzmann constant, and β is the attenuation coefficient of coal and rocks.

The energy source term is directly proportional to the fuel density through the heat release. Along with the fuel consumption, the density of the remaining coal that decreases gradually till the coal burns out is described as follows:

$$\rho_c = (1 - \int q(T)dt/Q_{\text{net}})\rho_s \tag{5}$$

where Q_{net} is the net calorific value of coal.

Coal oxidizing process is controlled by oxygen supplement or local concentration of oxygen. In this study, a maximum theoretical fuel consumption is defined as C_o/O_r, in which C_o in kg/m^3 is the local oxygen concentration and O_r in kg/kg is the theoretical oxygen requirement for combustion determined by elemental contents in coal [29]. If this maximum value is less than the calculated fuel consumption $\Delta\rho_c (= \rho_s \int_t^{t+\Delta t} q(T)dt/Q_{\text{net}})$ intergraded within Δt time, local coal consumption is replaced with the maximum value of theoretical fuel consumption and the oxygen concentration is set to be zero. Otherwise, the local value of oxygen consumption in coal seam is obtained by $O_r \times \Delta\rho_c$.

Furthermore, the oxygen distribution in the coal and rock medium is controlled by gas diffusion function or Fick law [13] as follows:

$$\varphi\frac{\partial C_o}{\partial t} + \vec{v}\cdot\nabla C_o - \varphi\nabla\cdot(D\nabla C_o) - w = 0 \tag{6}$$

where D ($= 2.05 \times 10^{-5}$ m^2/s) is the diffusion coefficient of oxygen air and w in kg/(m^3 s) represents the quantity of local oxygen consumption. Notice that both Eqs. (4) and (6) include an inertia term directly related to the velocity of seepage flow which was reported as an extremely small value [30]. In order to describe the seepage flow in porous medium, combined with ideal gas equation, the Darcy law [30], which reads $\vec{v} = -\frac{k}{\mu}\nabla p$, is involved in continuous equation that could be derived as follows:

$$S\frac{\partial p}{\partial t} - \frac{k}{\mu}\nabla\cdot\left(\nabla p - \rho_f\bar{g}\right) = 0 \tag{7}$$

where k in m^2 is the permeability in porous coal or rock, μ is air dynamic viscosity and set to be 1.8×10^{-5} Pa s, S is the compressibility which could be assumed as 10^{-5} Pa^{-1} [16], p is the hydrostatic pressure in Pa, and $\bar{g}$ in m/s^2 represents the gravitational vector.

3.2. Simulation

In practice, the fire area of small coal kilns in Anjialing open-pit mine in China is concerned as the study case. By utilizing room-pillar mining a horizontal array of open areas or "rooms" and coal pillars remained in the coal seam and there would exist a large strip bulk filled out huge amount of residual coals along the seam strike after coal kilns shutdown. In this circumstance, a two-dimensional simulation domain perpendicular to the ground for subsurface coal fire propagation is assumed and drawn in Figure 3. The horizontal coordinate represents the seam strike direction. According to the field geology of coal-bearing strata under mining conditions and combining with

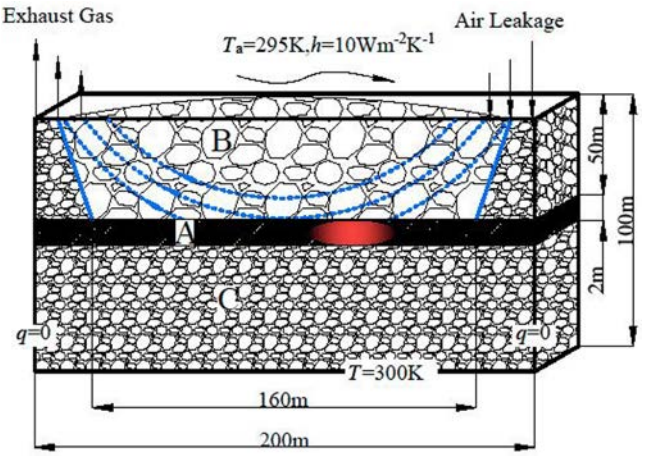

Figure 3. Sketch of the strata used in the present 2-D simulation. (Zone A: coal seam, Zone B: caved roof, Zone C: rock floor).

surface geophysical prospecting to coal fires, the length of settled line of surface electrical detection for coal fire delineating is about 200 m along the seam strike; therefore, the horizontal scale of simulating strata is set to be 200 m. A near-flat coal seam (zone A) about 2-m thick occurs in buried depth of 50 m, where a collapsed area of 160-m wide (consisted of several rooms and pillars) filled of loose coal after mining is considered and centered in the horizontal direction of the coal seam. Other portions of the seam are regarded as original stratum with massive coal. The whole height of the simulated strata from surface to the floor is assumed as 100 m. In addition, two main fracture channels exist at the edge of the top subsidence (zone B) caused by mining: the air flows into the crush rock from one side and the oxygen is supplied into uncovered coal seam by air seepage.

Considering field geological and mining conditions, the main chemical and thermophysical parameters employed in the modeling are presented as follows. By utilizing elemental analysis, the averaged contents of C, H, O, and S elements in coal C collected from the above coalfield region are 90.75, 2.48, 5.06, and 0.82 wt%, respectively; thus, the theoretical oxygen requirement for coal combustion is recorded as 2.576 kg/kg. The net calorific value of this measured coal sample is 30.97 MJ/kg. The averaged true relative density of local coal is around 1,800 kg/m^3. The upper stratum is mainly consisted with sandstone whose density varies from 2,300 to 2,700 kg/m^3 and the minimum value is employed here considering lightweight mudstone mixed in the rock roof. The porosity in stratum is directly related to the stress state of surrounding or occurrence depth. It is usually a small value. However, stratum porosity would greatly enhance after opening up [31]. In the simulation, the porosity in the uncovered coal seam (Zone A) and caved roof (Zone B) is assumed as 0.4 and 0.2, respectively, and it is regarded as 0.02 in the other unopened parts of the strata (Zone C). The permeability in coal and rock is directly determined by relevant porosity [32] and set to be 10^{-10}, 10^{-12}, and 10^{-18} m^2 in Zone A, B, and C, respectively. The specific heat capacity of rocks and air is assumed as 2.0 and 1.0 kJ/(kg K), respectively. The thermal conductivity of coal and rock is set as 0.2 and 2.0 W/(m K), respectively. The attenuation coefficient of the solid mass is assumed as 100 m^{-1} in the present simulation.

The boundary and initial conditions are defined below. For the temperature, an initial temperature at 300 K is assumed for all the zones in the strata. At the top surface, Robin boundary condition is applied for the surface considering convective heat transfer between rock and the ambient. Since the iteration step of simulation in this case study is usually set to 10 days during the coal self-heating development of several years, radiative heat transfer through the surface from solar or the earth irradiation day and night is ignored. The ambient temperature and convection coefficient are assumed 295 K and 10 W/(m^2 K), respectively. Considering the symmetric boundary on both sides

of the simulation domain, Neumann conditions are implemented and the diffusive flux of thermal energy is assumed zero. Since the deep layer below the domain could be regarded as invariable temperature stratum, Dirichlet condition is applied for the bottom boundary in which the temperature is assumed 300 K invariably.

For the fluid pressure, hydrostatic pressure distribution is considered initially for all the zones in the strata. The relevant pressure at a certain depth referred to standard barometric pressure of 101,325 Pa at surface is directly determined by local geopotential energy. The pressure for all the boundaries is assumed to be the reference value under Dirichlet condition. In addition, initial air density of 1.18 kg/m^3 at 300 K with oxygen content of 20 vol% is applied at the edge of the opened coal seam on the air entrance side as well as in the fracture channel.

The finite difference method with the implicit scheme is adopted in solving the coupled heat transfer equations, and the additional source term method is utilized to discrete boundary conditions. A rectangular gridding is carried on the simulation domain in which the general interval is set as 1 m. During simulation of any time step, Eq. (7) or fluid pressure distribution in the stratum is first solved with initial gas density, so that seepage velocity could be calculated by the Darcy law. Then, the oxygen distribution along the coal seam is obtained by solving diffusion Eq. (8) while the kinetic model is implemented to simulate the exothermic reaction and local fuel consumption in Eq. (6). Through comparing the oxygen requirement mentioned above, local oxygen or coal consumption and relevant heat release in the seam could be determined. The local porosity in the opened coal seam is dynamically corrected as the solid density reduces. If the local fuel burned out, the porosity at that position would be unity, representing the completely empty area filled out seepage air. After that, the heat transfer Eq. (4) would be solved to obtain temperature distribution. At the end, local gas densities for next iteration are updated by ideal gas equation and oxygen consumption.

4. Results and field validation

4.1. Thermal dynamic process

First of all, the two-stage oxidation kinetic parameters of the high rank coal (Coal C) consisted of 85.35% fixed carbon obtained by the synchronous thermal analysis introduced in Section 2 are implemented in the heat transfer calculation and the thermodynamic process of the subsurface coal fire development is evaluated. Based on the site geological and mining conditions of coal fire area in Anjialing coalfield, the geometrical, physical and chemical parameters presented in Section 3.2 are employed in the simulation.

Figure 4 plots the simulated temperature distributions in the 2-D strata model due to coal fire propagation at four time stages. The results show that the original temperatures in the coal and rook remain rather constant even 180 months (15 years) after coal uncovering. It means that the heat diffusion process and temperature rise in the coal is very slow in this early time stage. When the temperature in the oxidation core zone increases to over a critical value, a step change occurs in the thermal dynamic process in coal seam and the heating rate shows a geometric growth from time at 225 to 235 months. The combustion center first appears as a point-wise geometry and thereafter becomes elongated and then the elongated shape breaks down into two combustion centers that move in the up- and downward directions throughout the seam. The maximum temperature reaches to 1,545 K 235 months after by the upward moving fire, whereas the downward moving one exhibits a lower value.

Besides the temperature distributions, Figure 5 describes the relevant time-dependent slices of flow fields in the thermodynamic process. It is seen that since the permeability in the opened coal seam (Zone A) is two orders of magnitude higher than that in the roof (Zone B), on the preliminary oxidation stage (100 months after seam opening), leakage air mainly seeps into the collapsed coal area and chemisorption and oxygen consumption occur there by coal oxidation gradually. Meanwhile, the permeability in the original rock floor is very small so that the residual gases in the seam exhaust

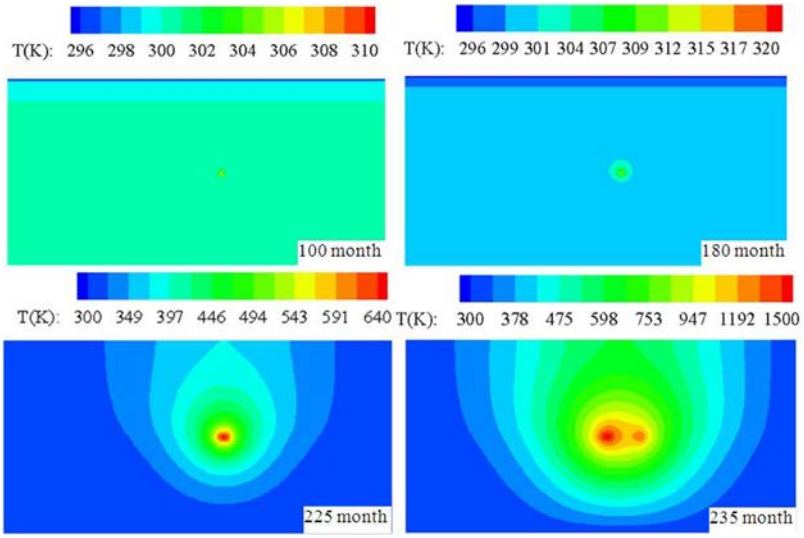

Figure 4. Simulated temperature distributions due to the underground coal fire at different time stages for Coal C with a two-stage kinetic model.

through the upper stratum into the atmosphere. After a long-term oxidation at low temperature or the first reaction stage with rich oxygen supplement, the hotspot in the seam caused by accumulating chemical and convective heat occurs and starts self-combusting. At the same time, the oxidizing reaction changes from the first stage to the second (235 months after seam opening up). Dramatic reactions consume oxygen rapidly and local fuel oxidation is under lean oxygen condition that means spontaneous heat process starts to be controlled by local oxygen concentration. With fire

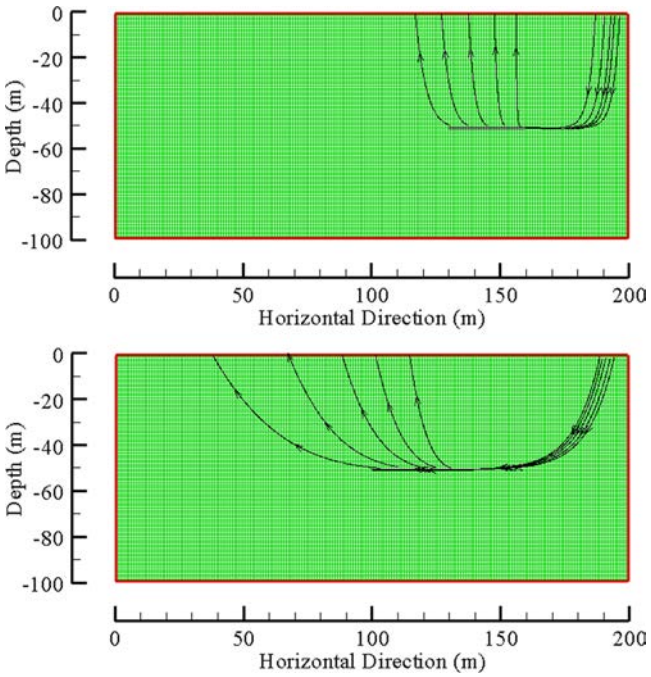

Figure 5. Simulated streamlines of seepage flow in a mined coal seam and collapsed floor (top: 100 months after coal uncovering, bottom: 235 months after coal uncovering).

development and fuel consumption, the leakage air seeps deeper into the seam because of enlarged empty area and heat-induced gas density variation. Combined with synchronous heat immigrations (see Figure 4), it is seen that the whole thermodynamic process of coal spontaneous combustion is real complex and developing under interactions of oxygen or fuel consumptions and coupled thermochemical transfer during different kinetic stages.

Figure 6 shows the temperature distributions for the locations below and above the coal seam as well as just at the surface at two different time stages. The temperature develops slowly above the ambient temperature. The distributions for both the below and above the coal seam locations are similar. Hence, the heat is not only released toward the surface, but also down into the rock. Meanwhile, the temperature below the seam is slightly smaller than that above the seam because of the different constraint conditions at the top and bottom boundaries. The pink vertical line coincides with the highest temperature and indicates the position of combustion core. Comparing the results at the two different time stages, it tells that the fire front is moving slowly after the coal self-ignition (roughly around 5 m every 10 months). The figure also shows that the horizontal positions with the highest temperature for above the seam and at the surface are inconsistent during the development of coal fire.

4.2. In-situ *survey and comparison*

In order to verify the rationality of the simulation results, a field survey of coal fire was carried out. The geophysical measurements have been conducted in the Anjialing open pit mine located in the Pinglu District of Shuozhou City in the Jinbei coal base (E112°18′36″-E112°29′24″, N39°27′00″-N39°34′12″) during March to June in 2013. The coal-bearing strata are the Taiyuan Formation of the Upper Carboniferous–Lower Permian and the Shanxi Formation of the Lower Permian–Middle Permian. The ground surface is covered by Cainozoic loess and there are 13 coal seams found in this area which occurring in the Taiyuan Formation. Most shallow-buried coal seams in this area are thick and had been over-exploited by many small coal mines in the last century. A relatively large proportion of coal was left in place in the abandoned gobs, which were mined by laggard room-pillar

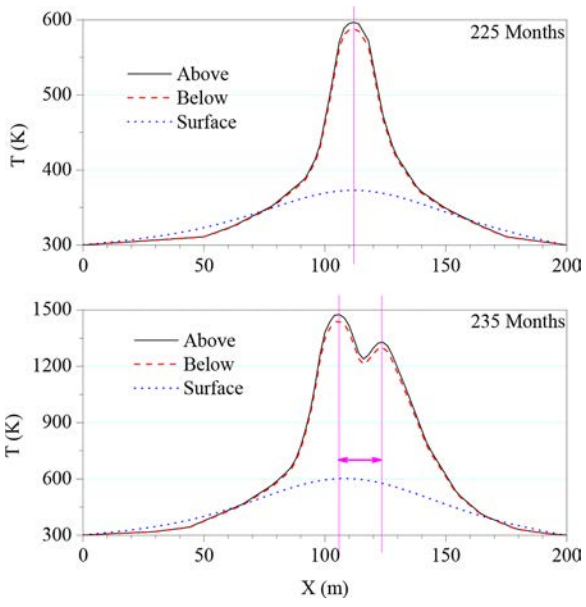

Figure 6. Simulated temperature distributions above and below the coal seam and at the surface for Coal C with a two-stage kinetic model.

mining. Without the sealing process after mine closeout, serious spontaneous combustion of residual coal occurred in these mine goafs and roadways. Due to stripping operation of the open-pit mine which caused the worsening of air leakage through the broken roof of small kiln, coal fires quickly developed to the depth level, resulting in a large-scale underground fire area in the Anjialing mining flat [33].

In order to delineate the coal fire area accurately by geophysical measurements and provide detailed references for validating the present numerical model, the high-density resistivity method was applied to fire detection. According to the surface conditions of Anjialing open-pit mine, 24 test lines were arranged with total detection length of 7920 m and the linear distance was set to be 20 m, while the minimum electrode distance was 5 m. The topography of the coal field with abandoned mines and a group test lines consisted of lines $21^{\#}$–$24^{\#}$ are drawn in Figure 7. After field measurement, the ground sampled data were processed by smoothness least squares inversion with Gauss-Newton iteration and transferred into pseudo resistivity tomograms for each detection line. By a comprehensive analysis of inversed resistivity profiles, surface delineation of coal fire area was obtained as shown in Figure 7, according to the resistivity anomalies induced by underground coal combustion.

It is seen that at the edge of estimated fire area, two boreholes A and B which lied on the survey line $24^{\#}$ and located at about 160.0 ± 0.5 m and 165.0 ± 0.5 m from the starting point of electrical detection in the southwest, respectively, were selected to measure the underground temperature around 50 m depth. The observation results of the two boreholes recorded in June 2013, December 2013, and June 2014 after electrical prospecting are compared with the simulated results in Figure 8. As mentioned above, the fire history of small-kiln coal mines can be traced as early as two decades ago and they were closed around the year 1997, and the borehole temperatures in June 2013 are consistent with the simulated results at about 216 months or 16 years from the beginning of residual coal oxidation. It demonstrates that the heat release and temperature rise of coal spontaneous combustion are quiet slow especially in the early stage. Simulation with the two-stage kinetic model could correctly describe a long developing process of underground smolder combustion of residual coal.

Furthermore, the measured temperatures of borehole A are higher than that of borehole B. This testifies the coal fire development toward the northeast. A corroborative evidence is that water vapor

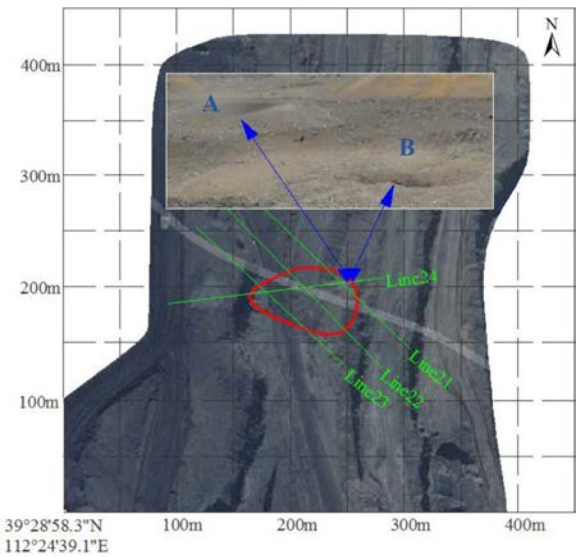

Figure 7. A portion topography of an Anjialing open-pit mine and geophysical surveys on small-kiln coal fire. The green lines denote the test lines of high-density resistivity detection. The red curve denotes the delineated area of coal fire. The blue triangles point to the temperature boreholes.

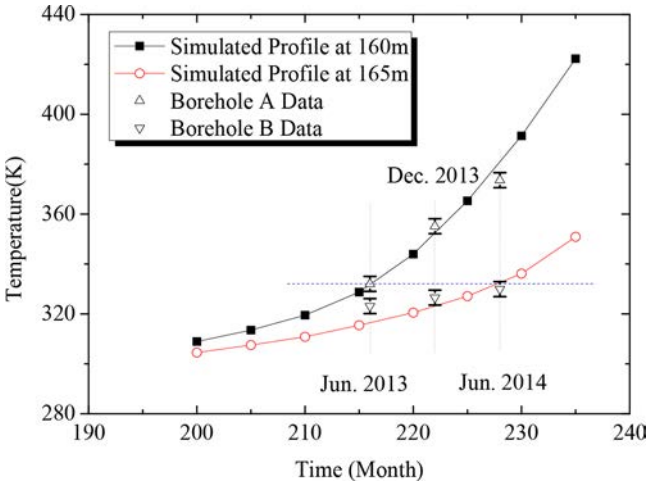

Figure 8. Comparison of the two-stage kinetics simulated temperature profiles for Coal C with the field observation data of two boreholes recorded in June 2013, December 2013, and June 2014, respectively.

and obvious smoke gradually appeared from the borehole A with the increase of drilling depth (cf. the field photo in Figure 6) while they were not observed in the other borehole. In Figure 8, it can be seen that the variation trend of the simulated temperatures at 160 m well inosculates with the profile of borehole A, and the data recorded in June 2014 are some lower than the simulation results. This difference due to the actual propagation of coal fire is still slower than the results of theoretical inferring. In fact, the temperature measured at borehole B in Jun. 2014 is even lower than that obtained at borehole A in Jun. 2013, that means the fire advance rate should be less than 5 m or might be around 3 m during the past year. In addition, other surveys on coal fires such as field magnetometer measurements [34] also have reported that the combustion front of underground coal fire advanced around 1 m every 5 months.

4.3. Effects of oxidation models

In order to reveal the distinctions between different oxidation kinetic models acting on coal fire development, Figure 9 compares the variations of maximum temperature in the strata of Coal C

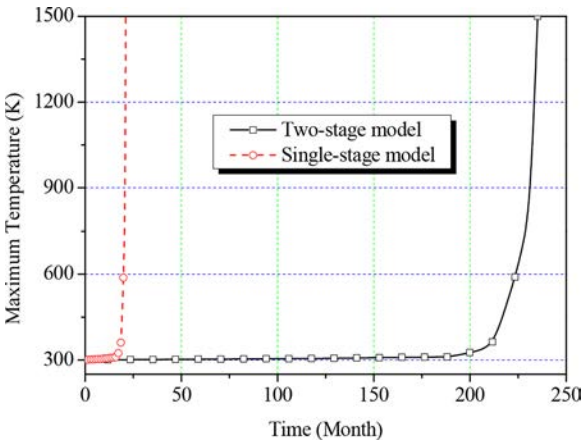

Figure 9. Comparison of the dynamical developments of maximum combustion temperature in strata predicted by different oxidation models.

predicted by the traditional single-stage kinetic model and by our two-stage kinetic model, respectively. As illustrated in the curve of the two-stage model, a liner and extremely slow increment of maximum temperature in the coal seam is obtained up to over 180 months after oxidation starts. When the oxidation temperature rises beyond the threshold value T_s as defined in Section 2, the chemical reaction process of coal is changing from the first-stage into the second-stage and the maximum temperature increasing rate proceeds much faster. It can be seen that the oxidation temperature is over the critical value after about 210 months and then the coal seam starts to self-ignite about 15 months later. In the last stage, the temperature rises from ignition to over 1,500 K in just 10 months. On the other side, the simulation with the single-stage kinetic model predicts that the coal fire processed in less than 2 years, which is quite different from the field observation in the last subsection and is nearly one order of magnitude shorter than that predicted by the two-stage model.

The differences of simulated results between the two kinetic models are further shown in Figure 10, in which the temperature distributions along the centerline of coal seam at different fire developing times are illustrated. The time for coal temperature reaching self-ignition predicted by the two-stage model is ten times of that predicted by the single-stage model. Using the single-stage model, it takes only 22 months for the coal temperature close to 1,500 K after coal ignition, while it spends around 235 months based on the two-stage model. Meanwhile, the coal fire zone of the single-stage model is much wider than that predicted by the two-stage model. The pink dash dot line in Figure 10 indicates the development of the fire front. It is seen that the fire propagation rate simulated by the single-stage model is much faster than that by using the two-step model. According to some previous reports in the literature and the present field survey, the combustion front of underground coal fire moves very slowly. Therefore, the present two-stage oxidation model is more adequate for predicting the long history of coal fire propagation and coincides better with the field observation.

4.4. Effects of the coal rank

As mentioned in Section 2, the kinetic parameters of activation energy and frequency factor determine the exothermic properties of coal oxidation and are dependent on the coal rank and

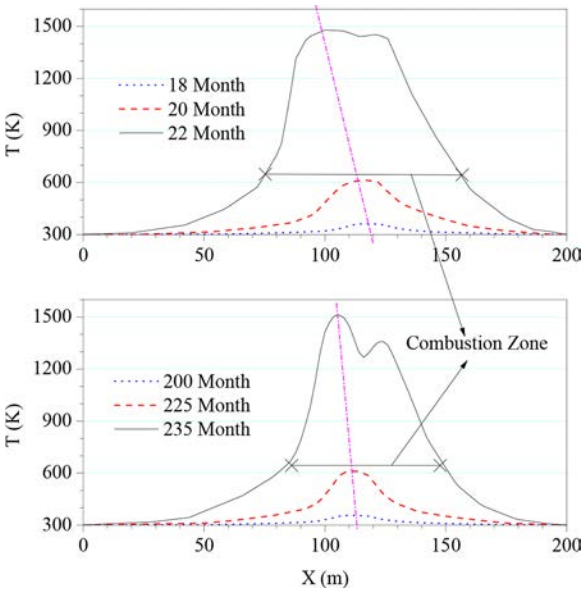

Figure 10. Temperature profiles at different times along the centerline of coal seam. (Top: single-stage model, bottom: two-stage model).

Table 1. Ultimate and proximate analyses of typical coal samples.

Coal sample		Coal A (Lignite)	Coal B (Bitumite)	Coal C (Anthracite)	Uncertainty
Ultimate analysis (wt%)	Moisture	7.88	2.53	6.05	±0.24
	Ash	3.97	4.08	0.64	±0.16
	Volatile matter	61.78	32.18	7.96	±0.40
	Fixed carbon	26.37	61.21	85.35	NA
Proximate analysis (wt%)	S	1.36	3.67	0.82	±0.06
	C	65.24	81.73	90.75	±0.23
	H	5.12	5.34	2.48	±0.07
	O	27.37	8.91	5.06	NA
	N	0.91	0.35	0.89	±0.05
Q_{net} (MJ/kg)		23.04	30.27	30.97	±0.18

Table 2. Oxidation kinetic parameters measured for the coal samples.

Coal sample	T_s(K)	T_m(K)	Reaction Stage	E_a (kJ/mol)	$QA \times 10^{-6}$ (kW/kg)
A	598.0 ± 4.2	683.0 ± 3.9	LOW	57.3 ± 1.6	0.34 ± 0.02
			HIGH	66.1 ± 1.9	1.21 ± 0.11
B	661.0 ± 2.8	778.0 ± 3.7	LOW	60.5 ± 1.5	1.29 ± 0.12
			HIGH	77.1 ± 2.3	2.34 ± 0.17
C	725.0 ± 4.7	844.0 ± 5.6	LOW	61.2 ± 2.1	3.80 ± 0.18
			HIGH	92.9 ± 3.4	10.0 ± 0.26

metamorphism. In order to study the effects of coal rank on the thermal dynamic process of coal fire, three kinds of typical coal obtained from different coalmines were considered, i.e., a high volatile lignite (Coal A), a bituminous coal (Coal B), and a high carbon content anthracite (Coal C). It means that sample A has the lowest rank while coal C has the highest rank. Indeed, the oxidation kinetic characteristics of sample C have been employed in all the foregoing simulations. The ultimate and proximate properties of these coal samples are measured in this study and listed in Table 1.

Based on the experiments described in Section 2, the kinetic parameters of these three samples in two oxidation stages are determined by using the synchronous thermal analysis. The measured activation energy E_a and reaction heat variable QA as well as the corresponding critical temperatures are listed in Table 2. It is remarkable that the data at temperature below the critical temperature T_s are much lower than those in the temperature range above this threshold temperature. It means that for any sample, the oxidation rate or heat release grows very slowly in the low-temperature range, but grows quickly after the coal temperature rises beyond the threshold temperature.

Using the two-stage reaction model and properties in Table 2, the heat transfer and thermodynamic processes for all three coal samples were conducted. Figure 11 compares the time developments

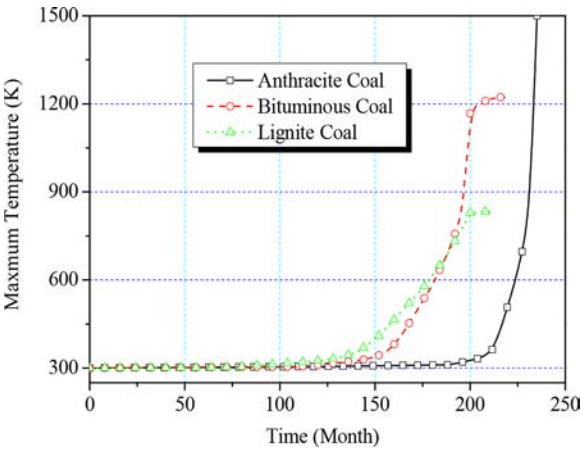

Figure 11. Comparison of the developments of maximum temperature in the coal seam of different rank coals.

of maximum temperature among the three coal samples. It is seen that the fire developing of the lowest rank coal seam (Lignite, Coal A) is the fastest one while a higher rank coal (Anthracite, Coal C) could achieve a higher temperature level. From Table 2, it is clear that the activation energy of the lowest rank sample is the lowest. It means that the oxidation process could occur earlier and more easily. On the other side, the highest rank coal has the largest heat release so that it could realize the highest maximum temperature in the thermodynamic process of coal fire.

5. Conclusions

Coal oxidation properties of three kinds of typical coals were measured by using the TG–DSC method and fitted into the two-stage kinetic model. A combined heat transfer model for porous coal and rocks was employed to simulate the temperature history and thermodynamic process in coal-bearing strata with the determined oxidation properties. Effects of oxidation kinetic feature due to coal metamorphism on propagation characteristics of coal fires were examined. The simulated temperature development was compared with field measurement and a reasonable agreement was found. The two-stage oxidation kinetic model was found to match with the slow growth of coal fires in field. While the traditional single-stage model predicted a much quick development of coal fires, nearly one-order of magnitude faster than the prediction of the two-stage model and the field geophysical prospecting.

The evaluated heat evolution during oxygen chemisorption and the kinetic parameters of the three typical coals under different temperature levels demonstrated that coal oxidation could be better described by a two-stage process separated by a critical threshold temperature, rather than by the typical single-stage model. The simulated results of the temperature distributions and the maximum combustion temperatures due to the underground coal fire at different times showed that the temperature of coal seam is nearly constant during a quite long period after mining. This is attributed to the slow oxidation process at low temperature. Coal fire ignites and starts to penetrate to the up- and downward directions through the seam when the oxidation switches into the second stage after passing the threshold temperature. In this stage, the fire develops quickly. It was found that the rank of coal has remarkable influence on coal fire propagation and maximum temperature that could be reached.

Funding

This research was supported by the Outstanding Youth Science Foundation of NSFC (No. 51522601), the National Natural Science Foundation of China (No. 51676206), and Program for New Century Excellent Talents in University (NCET-13-0173). Y.M. Wang appreciates the Scholarship provided by the Chinese Scholarship Council to study at Rutgers University.

References

[1] G. B. Stracher and T. P. Taylor, Coal Fires Burning Out of Control Around the World: Thermodynamic Recipe for Environmental Catastrophe, *Int. J. Coal Geol.*, vol. 59, pp. 7–17, 2004.
[2] A. E. Whitehouse and A. A. S. Mulyana, Coal Fires in Indonesia, *Int. J. Coal Geol.*, vol. 59, pp. 91–97, 2004.
[3] A. Rosema, H. Y. Guan, and H. Veld, Simulation of Spontaneous Combustion to Study the Causes of Coal Fires in the Rujigou Basin, *Fuel*, vol. 80, pp. 7–16, 2001.
[4] J. D. N. Pone, K. A. A. Hein, G. B. Stracher, H. J. Annegarn, R. B. Finkelman, and D. R. Blake, The Spontaneous Combustion of Coal and Its By-Products in the Witbank and Sasolburg Coalfields of South Africa, *Int. J. Coal Geol.*, vol. 72, pp. 124–140, 2007.
[5] B. Taraba, R. Peter, and V. Slovák, Calorimetric Investigation of Chemical Additives Affecting Oxidation of Coal at Low Temperatures, *Fuel Process. Technol.*, vol. 92, pp. 712–715, 2011.
[6] Y. M. Wang, W. Z. Wang, Z. L. Shao, D. M. Wang, and G. Q. Shi, Terahertz Measurement of Indicator Gas Emission from Coal Spontaneous Combustion at Low Temperature, *Ecol. Chem. Eng. S*, vol. 20, pp. 709–718, 2013.

[7] K. Yip, E. Ng, C. Z. Li, J. I. Hayashi, and H. W. Wu, A Mechanistic Study on Kinetic Compensation Effect During Low-Temperature Oxidation of Coal Chars, *Proc. Combust. Inst.*, vol. 33, pp. 1755–1762, 2011.
[8] S. Porada, The Influence of Elevated Pressure on the Kinetics of Evolution of Selected Gaseous Products During Coal Pyrolysis, *Fuel*, vol. 83, pp. 1071–1078, 2004.
[9] M. V. Gil, D. Casal, C. Pevida, J. J. Pis, and F. Rubiera, Thermal Behavior and Kinetics of Coal/Biomass Blends During Co-Combustion, *Bioresour. Technol.*, vol. 101, pp. 5601–5608, 2010.
[10] S. J. Zarrouk and M. J. O'Sullivan, Self-Heating of Coal: The Diminishing Reaction Rate, *Chem. Eng. J.*, vol. 119, pp. 83–92, 2006.
[11] J. C. Jones, K. P. Henderson, J. Littlefair, and S. Rennie, Kinetic Parameters of Oxidation of Coals by Heat-Release Measurement and Their Relevance to Self-Heating Tests, *Fuel*, vol. 77, pp. 19–22, 1998.
[12] M. X. Liu, G. Q. Shi, Z. X. Guo, Y. M. Wang, and L. Y. Ma, 3-D Simulation of Gases Transport under Condition of Inert Gas Injection into Goaf, *Heat Mass Transfer*, vol. 52, pp. 2723–2734, 2016.
[13] G. Q. Shi, M. X. Liu, Y. M. Wang, W. Z. Wang, and D. M. Wang, Computational Fluid Dynamics Simulation of Oxygen Seepage in Coal Mine Goaf with Gas Drainage, *Math. Probl. Eng.*, Article ID 723764, 9 pages, 2015. http://dx.doi.org/10.1155/2015/723764.
[14] Y. M. Wang, W. Z. Wang, Z. L. Shao, D. M. Wang, and G. Q. Shi, Innovative Prediction Model of Carbon Monoxide Emission from Deep Mined Coal Oxidation, *Bulg. Chem. Commun.*, vol. 46, pp. 887–895, 2014.
[15] J. J. Huang, J. Bruining, and K. Wolf, Modeling of Gas Flow and Temperature Fields in Underground Coal Fires, *Fire Saf. J.*, vol. 36, pp. 477–489, 2001.
[16] S. Wessling, C. Kuenzer, W. Kessels, and M. W. Wuttkea, Numerical Modeling for Analyzing Thermal Surface Anomalies Induced by Underground Coal Fires, *Int. J. Coal Geol.*, vol. 73, pp. 175–184, 2008.
[17] Y. M. Wang, G. Q. Shi, and D. M. Wang, Numerical Study on Thermal Environment in Mine Gob under Coal Oxidation Condition, *Ecol. Chem. Eng. S*, vol. 20, pp. 567–578, 2013.
[18] K. Wolf and J. Bruining, Modeling the Interaction between Underground Coal Fires and their Roof Rocks, *Fuel*, vol. 86, pp. 2761–2777, 2007.
[19] Z. Klika, T. Kozubek, P. Martinec, C. Kliková, and Z. Dostál, Mathematical Modeling of Bituminous Coal Seams Burning Contemporaneously with the Formation of a Variegated Beds Body, *Int. J. Coal Geol.*, vol. 59, pp. 137–151, 2004.
[20] A. G. Kim, Locating Fires in Abandoned Underground Coal Mines, *Int. J. Coal Geol.*, vol. 59, pp. 49–62, 2004.
[21] S. Biswas, N. Choudhury, P. Sarkar, A. Mukherjee, S. G. Sahu, P. Boral, and A. Choudhury, Studies on the Combustion Behavior of Blends of Indian Coals by TGA and Drop Tube Furnace, *Fuel Process. Technol.*, vol. 87, pp. 191–199, 2006.
[22] K. E. Ozbas, M. V. Kök, and C. Hicyilmaz, DSC Study of the Combustion Properties of Turkish Coals, *J. Therm. Anal. Calorim.*, vol. 71, pp. 849–856, 2003.
[23] S. R. Dhaneswar and S. V. Pisupati, Oxy-Fuel Combustion: The Effect of Coal Rank and the Role of Char-CO_2 Reaction, *Fuel Process. Technol.*, vol. 102, pp. 156–165, 2012.
[24] B. Li, G. Chen, H. Zhang, and C. Sheng, Development of Non-Isothermal TGA-DSC for Kinetics Analysis of Low Temperature Coal Oxidation Prior to Ignition, *Fuel*, vol. 118, pp. 385–391, 2014.
[25] P. Garcia, P. J. Hall, and F. Mondragon, The Use of Differential Scanning Calorimetry to Identify Coals Susceptible to Spontaneous Combustion, *Thermochim. Acta*, vol. 336, pp. 41–46, 1999.
[26] N. Himrane, D. E. Ameziani, K. Bouhadef, and R. Bennacer, Storage Silos Self Ventilation: Interlinked Heat and Mass Transfer Phenomenon, *Numer. Heat Transfer A - Appl.*, vol. 66, pp. 379–401, 2014.
[27] V. K. Mishra, S. C. Mishra, and D. N. Basu, Combined Mode Conduction and Radiation Heat Transfer in a Porous Medium and Estimation of the Optical Properties of the Porous Matrix, *Numer. Heat Transfer A - Appl.*, vol. 67, pp. 1119–1135, 2015.
[28] Y. S. Sun, J. Ma, B. W. Li, and Z. X. Guo, Prediction of Nonlinear Heat Transfer in a Convective-Radiative Fin with Temperature-Dependent Properties by the Collocation Spectral Method, *Numer. Heat Transfer B - Fund.*, vol. 69, pp. 68–83, 2016.
[29] B. K. Mazumdar, Theoretical Oxygen Requirement for Coal Combustion: Relationship with Its Calorific Value, *Fuel*, vol. 79, pp. 1413–1419, 2000.
[30] T. Ren, CFD Modelling of Longwall Goaf Gas Flow to Improve Gas Capture and Prevent Goaf Self-Heating, *J. Coal Sci. Eng.*, vol. 15, pp. 225–228, 2009.
[31] L. M. Yuan and A. C. Smith, Numerical Study on Effects of Coal Properties on Spontaneous Heating in Longwall Gob Areas, *Fuel*, vol. 87, pp. 3409–3419, 2008.
[32] Q. Zeng, T. Tiyip, M. W. Wuttke, and W. M. Guan, Modeling of the Equivalent Permeability for an Underground Coal Fire Zone, Xinjiang Region, China, *Nat. Hazards*, vol. 78, pp. 957–971, 2015.
[33] Z. L. Shao, D. M. Wang, Y. M. Wang, X. X. Zhong, X. F. Tang, and X. M. Hu, Controlling Coal Fires Using the Three-Phase Foam and Water Mist Techniques in the Anjialing Open Pit Mine, China, *Nat. Hazards*, vol. 75, pp. 1833–1852, 2015.
[34] T. S. Ide, N. Crook, and F. M. Orr, Magnetometer Measurements to Characterize a Subsurface Coal Fire, *Int. J. Coal Geol.*, vol. 87, pp. 190–196, 2011.